Supporting Information for

Two {Dy_2} single-molecule magnets formed *via* an in situ reaction by capturing CO_2 from atmosphere under ambient conditions

Kun Zhang,[a] Fu-Sheng Guo[a] and Yao-Yu Wang*[a]*

[a] *Key Laboratory of Synthetic and Natural Functional Molecule Chemistry of the Ministry of Education, Shaanxi Key Laboratory of Physico-Inorganic Chemistry, College of Chemistry & Materials Science, Northwest University, Xi'an, 710127 (P.R.China)*

e-mail: guofush@hotmail.com; wyaoyu@nwu.edu.cn

Supplementary Information Contents

General considerations: All reagents were purchased from commercial sources and used as received. Elemental analyses (C, H, N) were determined with an Elementar vario EL III Analyzer. The FT-IR spectra were recorded from KBr pellets in the range 4000-400 cm^{-1} on a Bruker Tensor 27 spectrometer. The magnetization data of complexes of **1** and **2** were recorded on a Quantum Design MPMS-XL, VSM SQUID magnetometer equipped with a 7 T magnet, respectively. Variable-temperature magnetization was measured with an external magnetic field of 500 Oe in the temperature range of 1.8–300 K and the frequency dependent ac susceptibility was measured with an oscillating field of 3.5 Oe for **1**, 2.0 Oe for **2**. Finely ground microcrystalline powder of **1 - 2** was immobilized in eicosane matrix inside a polycarbonate capsule. Both the contributions of the eicosan and the capsule have been subtracted from the data obtained. Phase purity was checked by powder X-ray diffraction (PXRD) using a Bruker AXS D8 Advance diffractometer with Cu-Kα (λ =1.54056 Å) radiation. The mass spectrometry data were collected using a Bruker microTOF-QII mass spectrometer. The spectrometer was previously calibrated with sodium formate by switching the sheath liquid to a solution containing 5 mM sodium hydroxide in the sheath liquid of 0.2% formic acid in water/isopropanol 1:1 v/v. The electrospray source was used with the drying nitrogen gas temperature at approx +180 ºC.

Synthesis of complex $[Dy_2(L)_2(DBM)_2(DMF)_2]$ (1). To a stirred solution of o-vanillin (30.4 mg, 0.2 mmol), hydrazine hydrate (85%, 0.01 mL, 0.2 mmol), dibenzoylmethane (HDBM 44.8 mg, 0.2 mmol), $Dy(NO_3)_3{\cdot}6H_2O$ (131.6 mg, 0.3 mmol), and triethylamine (0.08 ml, 0.6 mmol) in acetonitrile (MeCN)–dimethylformamide (DMF) (1:1, 10 ml). The resulting solution was stirred for one hour and filtered, and then the filtrate was allowed to stand at room temperature for two days. Yellow block-shaped crystals suitable for single crystal analysis were formed by slow evaporation of solvent and were collected by careful filtration (69% yield based on Dy). IR spectra (cm^{-1}): 3427 (m), 1658(s), 1597(s), 1554(s), 1520(s), 1456(s), 1390(s), 1269(m), 1221(m), 1147(m), 1082(m), 1032(m), 951(w), 849(w), 781(m), 731(m), 673(m), 609(w). Elemental analysis found (calc.)% for complex **1**: C: 48.37(48.62); H: 3.98(3.93); N: 6.18(6.30).

Synthesis of complex $[Dy_2(L)_2(DBM)_2(DMA)_2]$ (2). Complex **2** was synthesized according to a similar process for that of complex **1**, except using the dimethylacetamide (DMA) as starting solvent instead of dimethylformamide (DMF). The resulting solution was stirred for one hour and filtered, and then the filtrate was allowed to stand at room temperature for two days. Yellow block-shaped crystals suitable for single crystal analysis were formed by slow evaporation of solvent and were collected by careful filtration (53% yield based on Dy). IR spectra (cm^{-1}): 3419 (m), 3188(m), 2949(m), 1653(s), 1601(s), 1554(s), 1520(s), 1456(s), 1392(s), 1267(s), 1219(s), 1147(s), 1084(s), 1030(s), 951(m), 849(w), 781(s), 729(s), 692(m), 600(m),534(w), 519(w). Elemental analysis found (calc.)% for complex **2**: C: 49.26(49.38); H: 4.02(4.14); N: 6.09(6.17).

Comparable synthesis experiments of complex 1 (in presence or absence of CO_2). A 50 mL Schlenk tube containing $Dy(NO_3)_3 \cdot 6H_2O$ (131.6 mg, 0.3 mmol), dibenzoylmethane (HDBM 44.8 mg, 0.2 mmol) and o-vanillin (30.4 mg, 0.2 mmol) was degassed under high vacuum (1-2 $\times 10^{-3}$ mbar) at room temperature for one hour, which followed by the addition of dried triethylamine (0.08 ml, 0.6 mmol) and MeCN : DMF (1:1, 10 ml). After stirring the solution under vacuum at room temperature for 30 min, the solution was charged with 1 atm CO_2. The yellow clear solution was then allowed to stand at room temperature and block crystals (namely **1a**) were formed at the bottom of the tube after 12 hours. IR, elemental analysis and powder X-ray diffraction confirmed that the block crystals is complex **1**. In contrast, repeating the same procedure without filling with CO_2 resulted in no crystals after two days. Note: Reactions were carried out in a Schlenk tube under Nitrogen atmosphere. IR spectra (cm^{-1}) for **1a**: 3421 (m), 1652(s), 1593(s), 1549(s), 1518(s), 1458(s), 1392(s), 1273(m), 1224(m), 1149(m), 1078(m), 1036(m), 950(w), 849(w), 783(m), 731(m), 671(m), 598(w). Elemental analysis found (calc.)% for complex **1a**: C: 48.51(48.62); H: 3.88(3.93); N: 6.38(6.30).

In addition, in order to probing the role of others reactants in the reaction between hydrazine and CO_2, we also conducted a comparable experiment repeating the same above procedure in presence of CO_2 but in the absences of HDBM, $Dy(NO_3)_3$ and triethylamin. Unfortunately, besides no crystals obtained after one day, we analyzed the reaction solution through ESI-MS and could not find and identify any peaks related to the new organic ligand, which indicate that the HDBM, $Dy(NO_3)_3$ and triethylamin play an indispensable role in completing the reaction between hydrazine and CO_2 (Figure S1).

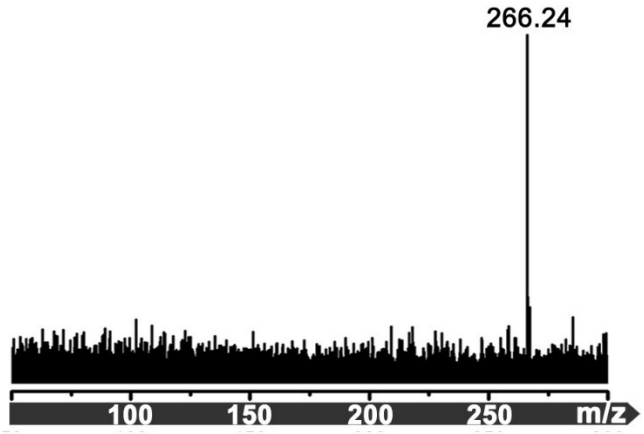

Figure S1. The mass spectrometry analysis of reaction solution of comparable synthesis experiments of complex **1** (in presence of CO_2 but in the absences of HDBM, $Dy(NO_3)_3$ and triethylamin). This solution was diluted 10:1 with methanol, and the data were collected in positive-ion mode.

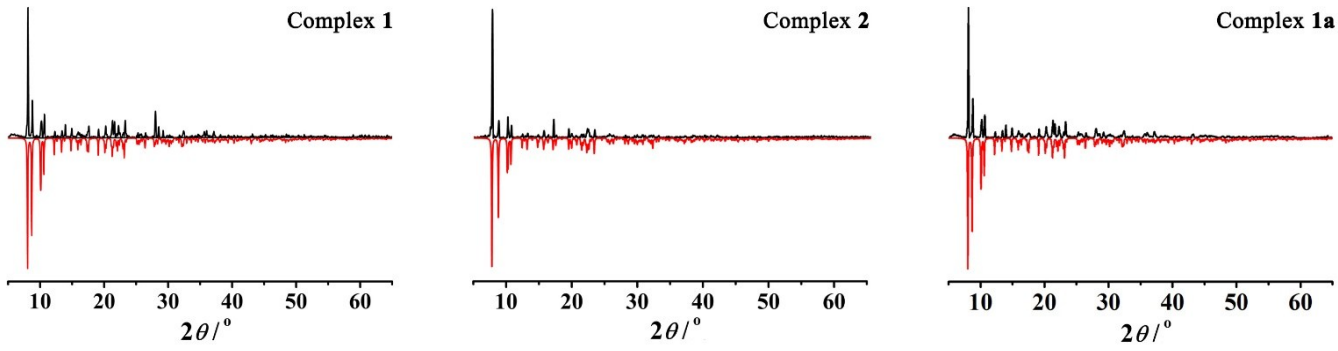

Figure S2. The experimental (black) powder X-ray diffraction and simulated patterns (red) of **1**, **2** and **1a**.

Electrospray Mass Spectrometry Study

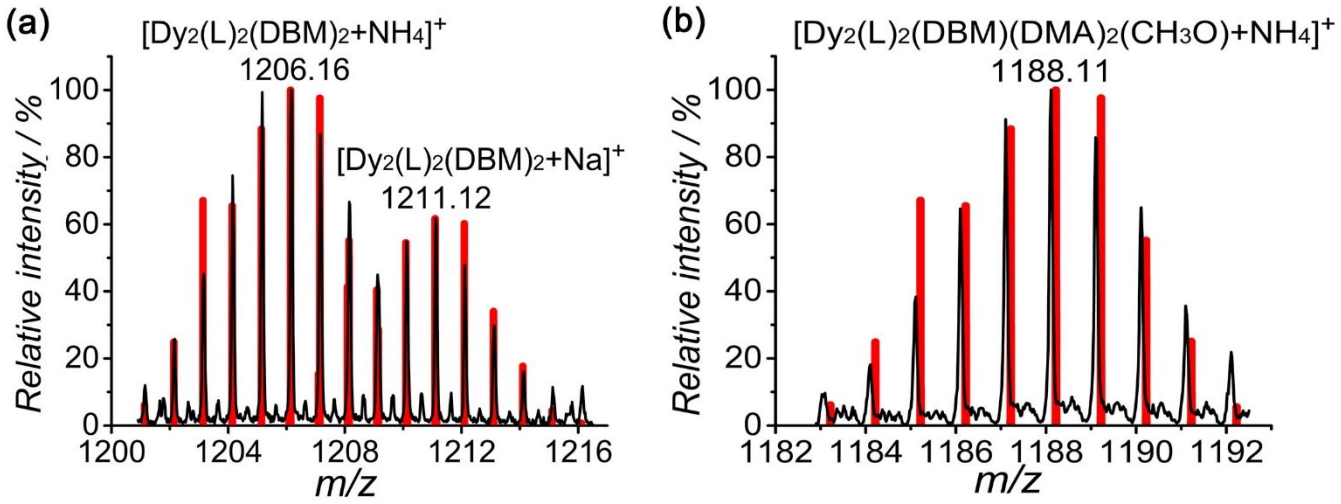

Figure S3. The mass spectrometry analysis of **1** and **2** is performed after few single crystals of **1-2** dissolved in 1 mL methanol for 10 mins. This solution was diluted 10:1 with methanol, and the data were collected in positive-ion mode. Red bars correspond to the simulated mass spectrometry data and black lines correspond to the experimental mass spectrometry data for complexes **1** (a) and **2** (b). All calculated peaks fit the statistical treatment of experimental error.

Note: Ionisation of a neutral analyte often occurs by cationisation, with an adventitious cation present in the solvent used, such as Na^+, NH_4^+. Such cations are present in solvents, especially polar solvents, which have been stored in glass bottles.[S1] In our case, the Na^+ , NH_4^+ ion could be introduced during the reaction process when the reactants kept in glass bottles, or the process of calibration for ESI instrument, which was performed using the sodium formate, may also introduce sodium ions.

[S1] W. Henderson and J. S. McIndoe, *Mass Spectrometry of Inorganic, Coordination and Organometallic Compounds: Tools - Techniques - Tips*, John Wiley & Sons, Chichester, 2005.

X-ray Crystallography Study

Single-crystal X-ray diffraction measurements for complexes **1** and **2** were carried out on a Bruker Apex II CCD diffractometer with graphite monochromated MoKα radiation (λ = 0.71073 Å) at 296 K. The structures were solved using the direct method (SHELXS) and refined by means of the full-matrix least-squares method (SHELXL) on F^2.[S2-S3] Anisotropic thermal parameters were used for the non-hydrogen atoms and isotropic parameters for the hydrogen atoms. Hydrogen atoms were added geometrically and refined using a riding model. Crystallographic data and refinement details are given in Table S1. CCDC 1510423 (**1**) and 1510424 (**2**).

[S2] G. M. Sheldrick, SHELXS-2014, Program for Crystal Structure Solution, University of Göttingen, 2014.

[S3] G. M. Sheldrick, *Acta Cryst. A*., 2008, **64**, 112-122.

Table S1. Summary of the Crystal Data and Structure Refinement Parameters for complexes **1** and **2**.

Complex	**1**	**2**
Formula	$C_{54}H_{52}Dy_2N_6O_{14}$	$C_{56}H_{56}Dy_2N_6O_{14}$
Fw	1334.01	1362.06
Crystal system	Monoclinic	Monoclinic
Space group	$P2_1/n$	$P2_1/n$
a (Å)	12.2677(16)	12.6016(12)
b (Å)	12.8118(17)	12.8099(12)
c (Å)	17.181(2)	17.3797(17)
α (°)	90.00	90.00
β (°)	103.489(2)	106.340(1)
γ (°)	90.00	90.00
Volume (Å^3)	2625.8(6)	2692.2(4)
Z	2	2
D_{calc} (g cm^{-3})	1.687	1.680
μ (mm^{-1})	2.896	2.827
F (000)	1324	1356
R_{int}	0.0319	0.0229
R_{sigma}	0.0406	0.0287
Refl. (all)	5094	5227
Refl. (> 2σ)	3958	4401
R_1 (all)	0.0516	0.0377
wR_2 (all)	0.0944	0.0780
R_1(> 2σ)	0.0349	0.0290
wR_2(> 2σ)	0.0842	0.0716
GOF.	1.058	1.088

$R_1 = \sum||Fo|-|Fc||/\sum|Fo|$, $wR_2 = [\sum w(Fo2-Fc2)2/\sum w(Fo2)2]^{1/2}$

Table S2 Selected bond lengths (Å) and angles (°) for complexes **1** and **2**.

1		**2**	
Dy1-O1	2.316(4)	Dy1-O1	2.348(2)
Dy1-O1[a]	2.366(3)	Dy1-O1[a]	2.371(2)
Dy1-O2	2.278(4)	Dy1-O2	2.281(3)
Dy1-O4[a]	2.485(4)	Dy1-O4[a]	2.510(3)
Dy1-O5	2.278(3)	Dy1-O5	2.282(3)
Dy1-O6	2.290(4)	Dy1-O6	2.303(3)
Dy1-O7	2.393(3)	Dy1-O7	2.366(3)
Dy1-N1	2.493(4)	Dy1-N1	2.487(3)
Dy1-O1-Dy1[a]	106.55(14)	Dy1-O1-Dy1[a]	106.16(10)
O1-Dy1-O1[a]	73.45(12)	O1-Dy1-O1[a]	73.84(9)
Symmetry transformations used to generate equivalent atoms : for **1**, a: 2-x, -y, 2-z; for **2**, a: 2-x, -y, 2-z.			

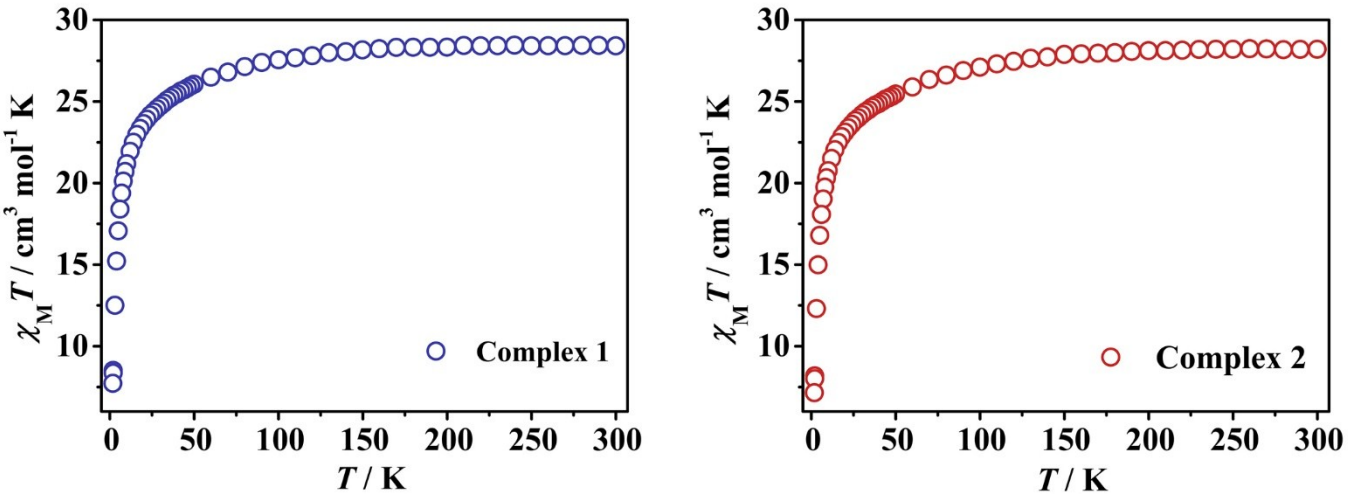

Figure S4. Plots of the $\chi_M T$ versus temperature for complex **1** and **2** in an applied magnetic field of 0.5 kOe.

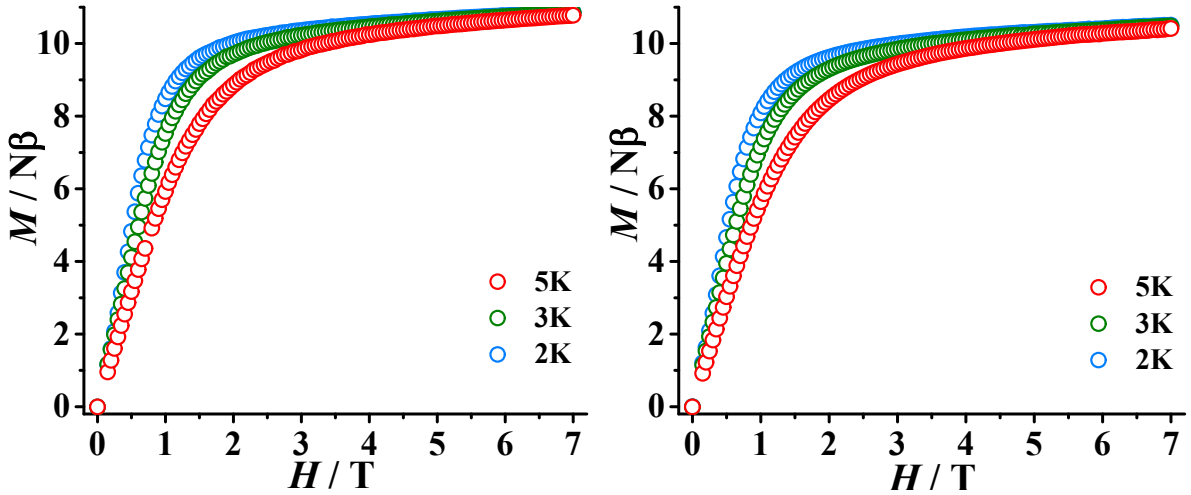

Figure S5. Field dependence of the magnetization, *M*, at 2, 3 and 5 K for complexes **1** and **2** plotted as *M vs. H*.

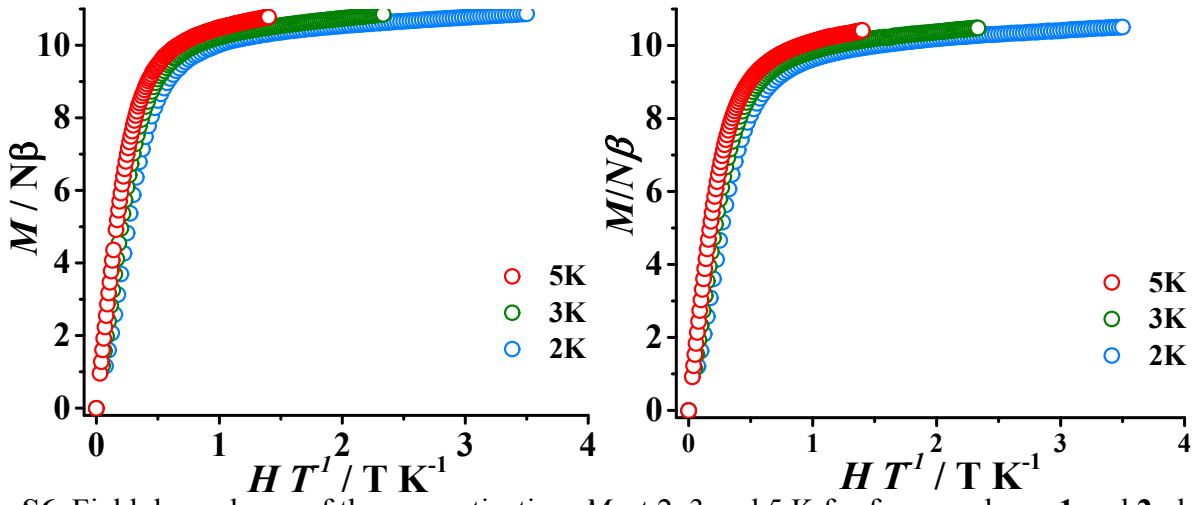

Figure S6. Field dependence of the magnetization, *M*, at 2, 3 and 5 K for for complexes **1** and **2** plotted as *M vs. HT*$^{-1}$.

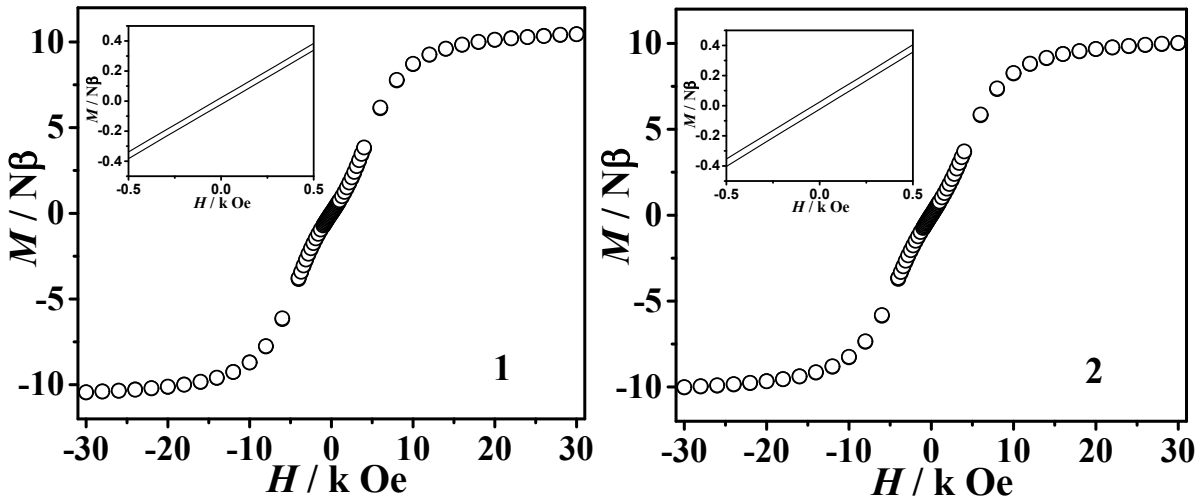

Figure S7. Magnetic hysteresis loops for complexes **1** and **2** with a sweep rate of 50 Oe s^{-1} at 1.8K.

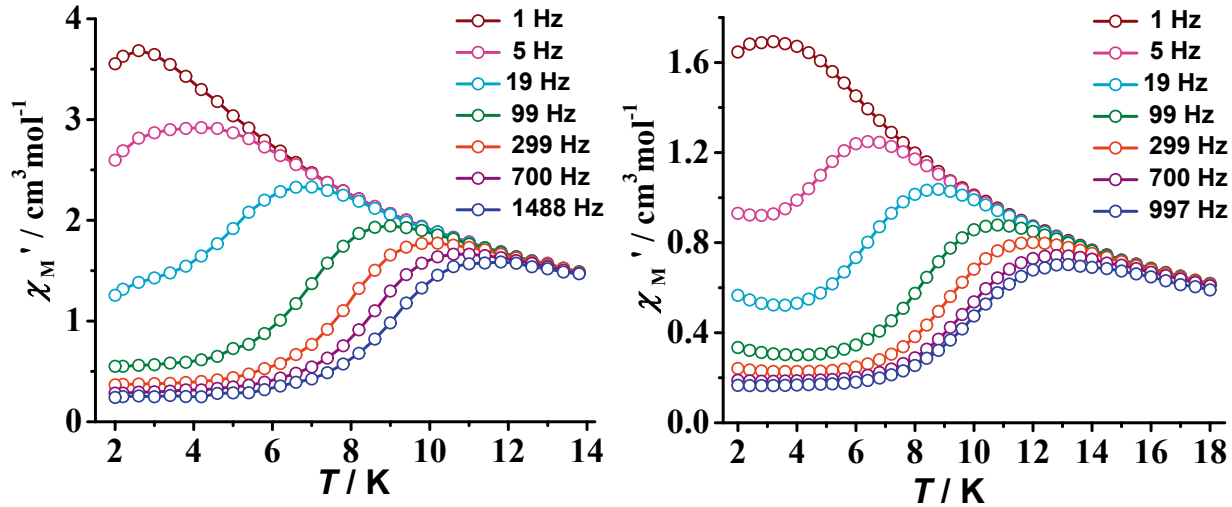

Figure S8. Temperature dependence under zero-dc field of the in-phase (χ') ac susceptibility component at different ac frequency for **1** (left) and **2** (right).

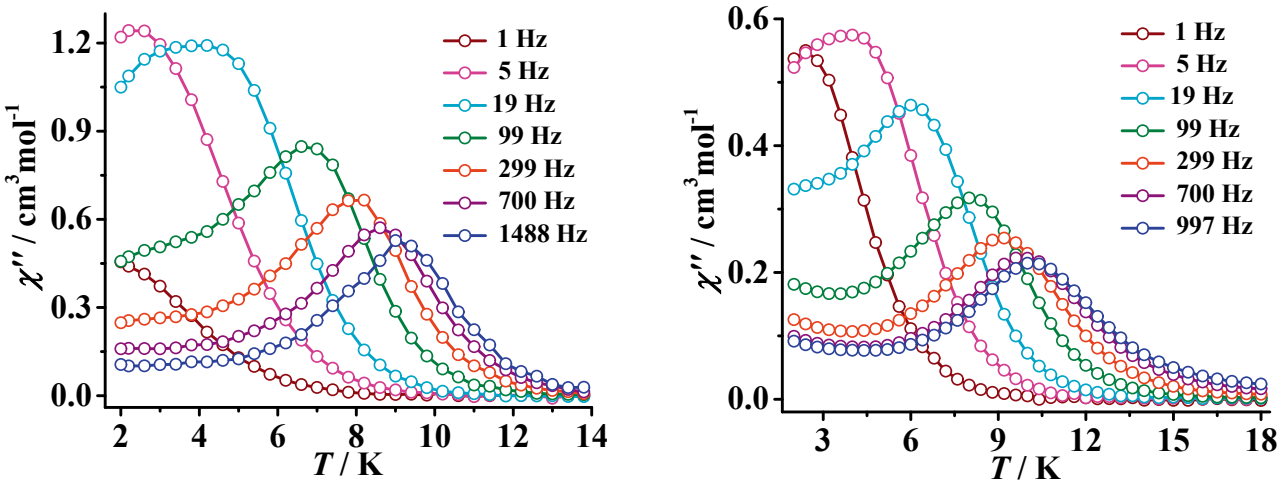

Figure S9. Temperature dependence under zero-dc field of the out-phase (χ'') ac susceptibility component at different ac frequency for **1** (left) and **2** (right).

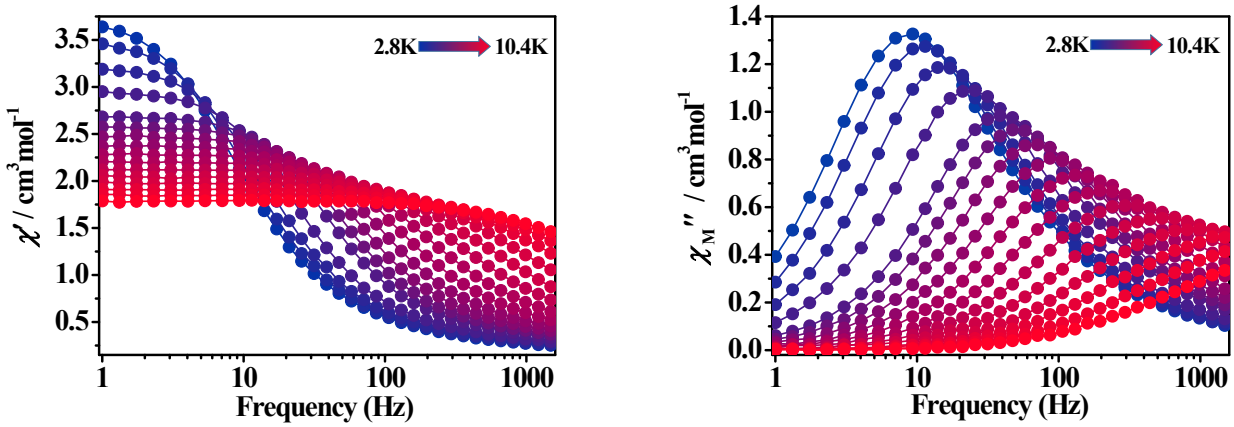

Figure S10. Frequency dependence in zero dc field of the in-phase (χ', left) and the out-of-phase (χ'', right) ac susceptibility component at different temperature for **1**.

Table S3. Relaxation fitting parameters from Least-Squares Fitting of $\chi(f)$ between 1-1488 Hz data under zero dc field of complex **1**.

Temperature	χ_T	χ_s	α	τ
2.8K	3.91	0.28	0.20	0.016
3.6K	3.64	0.29	0.18	0.013
4.4K	3.31	0.30	0.16	0.009
5.2K	3.02	0.31	0.14	0.006
6.0K	2.74	0.35	0.13	0.004
6.4K	2.62	0.37	0.13	0.003
6.8K	2.51	0.38	0.13	0.002
7.2K	2.41	0.40	0.14	0.001
7.6K	2.31	0.43	0.15	0.001
8.0K	2.23	0.45	0.17	6.95E-4
8.4K	2.14	0.48	0.18	4.58E-4
8.8K	2.06	0.51	0.20	2.94E-4
9.2K	1.99	0.56	0.21	1.91E-4
9.6K	1.92	0.59	0.22	1.21E-4
10.0K	1.86	0.67	0.22	8.30E-5
10.4K	1.79	0.78	0.22	6.16E-5

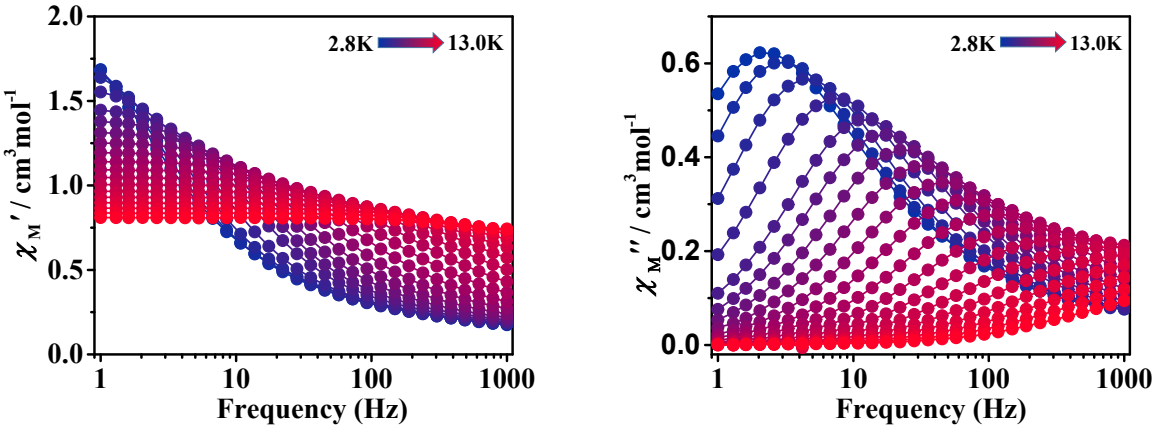

Figure S11. Frequency dependence in zero dc field of the in-phase (χ', left) and the out-of-phase (χ'', right) ac susceptibility component at different temperature for **2**.

Table S4. Relaxation fitting parameters from Least-Squares Fitting of χ(*f*) between 1-997 Hz data under zero dc field of complex **2**.

Temperature	χ_T	χ_s	α	τ
2.8K	2.54	0.16	0.39	0.082
3.6K	2.22	0.18	0.33	0.054
4.4K	1.93	0.19	0.28	0.032
5.2K	1.70	0.19	0.24	0.019
6.0K	1.53	0.19	0.22	0.011
6.5K	1.44	0.20	0.21	0.008
7.0K	1.36	0.20	0.21	0.006
7.5K	1.29	0.21	0.22	0.004
8.0K	1.23	0.22	0.23	0.002
8.5K	1.17	0.24	0.25	0.002
9.0K	1.11	0.25	0.26	0.001
9.5K	1.06	0.27	0.28	7.09E-4
10.0K	1.02	0.29	0.28	4.48E-4
10.5K	0.98	0.31	0.29	2.86E-4
11.0K	0.94	0.34	0.29	1.87E-4
11.5K	0.90	0.36	0.28	1.26E-4
12.0K	0.87	0.38	0.28	8.32E-5
12.5K	0.84	0.37	0.27	5.37E-5
13.0K	0.81	0.34	0.27	3.25E-5